IOWA STATE UNIVERSITY
Digital Repository

Electrical and Computer Engineering Publications

Electrical and Computer Engineering

3-13-2020

Fourier Analysis of Signal Waveforms in An Ideal Concurrent Dual-Band Class-D Power Amplifier

Subhanwit Roy
Iowa State University, roys@iastate.edu

Nathan Neihart
Iowa State University, neihart@iastate.edu

Follow this and additional works at: https://lib.dr.iastate.edu/ece_pubs

 Part of the Signal Processing Commons

The complete bibliographic information for this item can be found at https://lib.dr.iastate.edu/ece_pubs/246. For information on how to cite this item, please visit http://lib.dr.iastate.edu/howtocite.html.

This Article is brought to you for free and open access by the Electrical and Computer Engineering at Iowa State University Digital Repository. It has been accepted for inclusion in Electrical and Computer Engineering Publications by an authorized administrator of Iowa State University Digital Repository. For more information, please contact digirep@iastate.edu.

Fourier Analysis of Signal Waveforms in An Ideal Concurrent Dual-Band Class-D Power Amplifier

Abstract

Recently, a concurrent dual-band class-D power amplifier has been demonstrated to overcome the limitations of reduced efficiency in concurrent dual-band linear power amplifiers. However, the configuration could not be symbolically analyzed like its single-band counterpart due to the complicated nature of dual-band signals. This paper aims to provide a theoretical basis for idealized concurrent dual-band class-D operation. It applies an alternate representation of the sum of two sinusoids which helps the formulation of a technique to analytically extract the complex Fourier series coefficients of the current and voltage waveforms of the power amplifier. Expressions for output power and efficiency are derived, showing a theoretical drain efficiency of 100%. The theoretically obtained results are validated using observations from literature as well as independent Harmonic Balance simulation.

Keywords

Carrier Aggregation, Class-D, Complex Fourier Series, Concurrent Dual-band, Power Amplifiers.

Disciplines

Electrical and Computer Engineering | Signal Processing

Comments

This is a manuscript of an article published as Roy, Subhanwit, and Nathan M. Neihart. "Fourier Analysis of Signal Waveforms in An Ideal Concurrent Dual-Band Class-D Power Amplifier." *IEEE Transactions on Circuits and Systems II: Express Briefs* (2020). DOI: 10.1109/TCSII.2020.2980732. Posted with permission.

This article is available at Iowa State University Digital Repository: https://lib.dr.iastate.edu/ece_pubs/246

Fourier Analysis of Signal Waveforms in An Ideal Concurrent Dual-Band Class-D Power Amplifier

Subhanwit Roy, *Student Member, IEEE,* and Nathan M. Neihart, *Senior Member, IEEE*

***Abstract*—Recently, a concurrent dual-band class-D power amplifier has been demonstrated to overcome the limitations of reduced efficiency in concurrent dual-band linear power amplifiers. However, the configuration could not be symbolically analyzed like its single-band counterpart due to the complicated nature of dual-band signals. This paper aims to provide a theoretical basis for idealized concurrent dual-band class-D operation. It applies an alternate representation of the sum of two sinusoids which helps the formulation of a technique to analytically extract the complex Fourier series coefficients of the current and voltage waveforms of the power amplifier. Expressions for output power and efficiency are derived, showing a theoretical drain efficiency of 100%. The theoretically obtained results are validated using observations from literature as well as independent Harmonic Balance simulation.**

***Keywords*—Carrier Aggregation, Class-D, Complex Fourier Series, Concurrent Dual-band, Power Amplifiers**

I. Introduction

The burgeoning need to enhance data rates and data capacity of mobile networks, in modern times, are making operators turn toward combining carriers in different frequency bands. Non-contiguous carrier aggregation (CA) has been supported by LTE-Advanced [1] and is also a specification of 5G NR [2]. It has recently led researchers to look for concurrent multiband power amplifiers (PAs), which are capable of supporting multiple carrier frequencies simultaneously [3-6]. There are several challenges to designing concurrent multiband PAs that have been observed in the literature. Chief among these problems are a reduced efficiency and output power when compared to their single-band counterparts [7]. Taking a page out of the book of single-band PA designs, researchers have recently demonstrated a switch-mode class-D configuration to obtain high efficiency out of a dual-band PA [4, 8].

Even though the concurrent dual-band class-D PA has shown good performance empirically [4], it has not rendered well to symbolic analysis, compelling authors to curtail theory in lieu of direct numerical computation, as is often the case with complex PA designs [9]. On the other hand, an ideal single-band class-D PA can be analyzed using Fourier series with relative ease [10]. This is because the basis for such an analysis is formulating the zero-crossings of the input signal, which is straightforward for a single sinusoid (every half-cycle). However, the same does not apply for a signal which is the sum of two sinusoids at different frequencies, making the analysis of the dual-band PA much more complicated.

In this paper, we apply an alternate representation of the superposition of waves [11] to develop a technique to obtain the complex Fourier series of the current and voltage waveforms in an ideal concurrent dual-band transformer-coupled current-switching class-D PA. The developed theory is then used to derive the 100% ideal drain efficiency of such a configuration. We further demonstrate the utility of the analysis by analytically investigating the deterioration of the PA's efficiency under nonideal common-mode termination conditions [8]. Finally, we validate our theory using Harmonic Balance simulation.

II. Ideal Concurrent Dual-band Push-pull Class-D PA

The circuit of the ideal concurrent dual-band push-pull transformer-coupled current-switching class-D power amplifier is illustrated in Fig. 1. To appreciate pure class-D operation from a theoretical perspective, the transistors are assumed to be ideal switches, with zero ON resistance, infinite OFF resistance, and instantaneous switching time. In addition, the transistors are assumed to be perfectly linear with zero knee voltage. The inputs to the two transistors are defined to be:

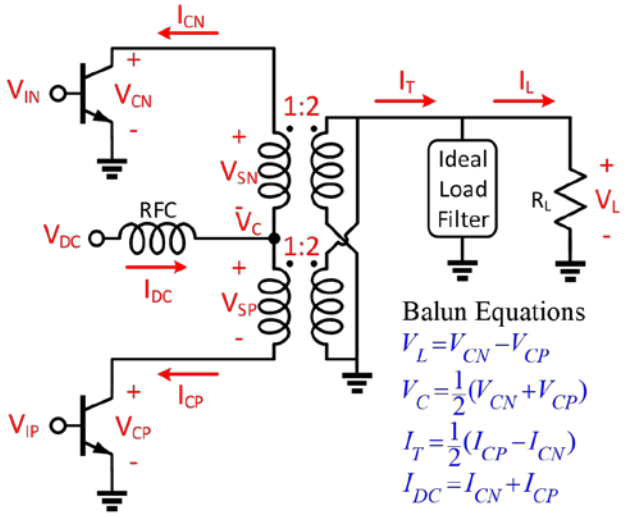

Fig. 1. Schematic of ideal push-pull concurrent dual-band class-D PA along with equations describing current and voltage relationships in balun.

Manuscript received January 30, 2020; accepted March 7, 2020. This work was supported in part by the National Science Foundation under grant number 1509001.

Subhanwit Roy and Nathan M. Neihart are with the Department of Electrical and Computer Engineering, Iowa State University, Ames, IA, 50011 USA.

$$V_{IN}(t) = \cos(\omega_L t) + \cos(\omega_H t) \quad (1)$$

$$V_{IP}(t) = -[\cos(\omega_L t) + \cos(\omega_H t)] \quad (2)$$

where ω_L and ω_H are the two angular frequencies of interest, such that $\omega_L < \omega_H$ and that f_L and f_H are both integers with $f_L = \omega_L / (2\pi)$ and $f_H = \omega_H / (2\pi)$. The RF choke inductor (RFC) is assumed to have infinite inductance and forces a constant current, I_{DC} to flow through it. An ideal lumped-element balun is assumed, consisting of two ideal transformers, each with turns ratio 1:2. The "Ideal Load Filter" seen in Fig. 1 is an ideal brickwall filter which perfectly passes frequency components at the two signal frequencies ω_L and ω_H, and perfectly rejects all other frequency components. Finally, it is assumed that the load impedance is purely real.

Having described the ideal PA circuit and the corresponding assumptions, we now proceed with the theoretical analysis. The RF choke enforces current-switched class-D operation. The current through each transistor will be equal to I_{DC} when the transistor is ON and zero when the transistor is OFF. This is expressed mathematically using the signum function as:

$$I_{CP}(t) = \frac{I_{DC}}{2} + \frac{I_{DC}}{2}\text{sgn}[\cos(\omega_L t) + \cos(\omega_H t)] \quad (3)$$

$$I_{CN}(t) = \frac{I_{DC}}{2} - \frac{I_{DC}}{2}\text{sgn}[\cos(\omega_L t) + \cos(\omega_H t)] \quad (4)$$

The collector currents, I_{CP} and I_{CN}, are combined using the balun relationship from Fig. 1, to give the unbalanced output current which can be expressed in terms of $V_{IN}(t)$ using (1):

$$I_T(t) = \frac{I_{DC}}{2}\text{sgn}[\cos(\omega_L t) + \cos(\omega_H t)] = \frac{I_{DC}}{2}\text{sgn}[V_{IN}(t)] \quad (5)$$

which is a square-wave alternating between $\pm I_{DC}/2$ with the same zero-crossings and period as the input signal described in (1). $I_T(t)$ is filtered by the ideal load filter before being applied to the load. Therefore, to calculate the amplitude of the current and voltage at the load, we will need to derive the complex Fourier series coefficients of $I_T(t)$. Also, once the load voltage is found, we can reflect it back across the balun to calculate the collector voltages, and use the balun expression for common-mode voltage to find its Fourier coefficients, and thus the value of V_{DC}, in a similar fashion to how a single-band transformer-coupled current-switched class-D PA is analyzed [12]. However, unlike the single-band case, direct extraction of the Fourier coefficients of (5) is nontrivial. This is because we do not know *a priori* the time instants when the direction of $I_T(t)$ changes, as opposed to the single-band PA, where the direction switches every half-cycle. Hence, to allow us to analytically compute the complex Fourier series coefficients of $I_T(t)$, we will introduce an alternate mathematical representation of the sum of sinusoids.

III. Mathematical Representation of a Sum of Sinusoids

Using expressions derived by Lord Rayleigh back in 1877 [11], and investigated more recently in [13], (1) can be written as an amplitude and phase modulated sinusoid, given by:

$$V_{IN}(t) = r(t)\cos(\omega_H t - \theta(t)) \quad (6)$$

where, defining $\omega_m = \omega_H - \omega_L$,

$$r(t) = \left|\sqrt{2(1+\cos(\omega_m t))}\right| = \left|2\cos\left(\frac{\omega_m t}{2}\right)\right| \quad (7)$$

$$\theta(t) = \tan^{-1}\left(\frac{\sin(\omega_m t)}{1+\cos(\omega_m t)}\right) = \tan^{-1}\left(\tan\left(\frac{\omega_m t}{2}\right)\right) \quad (8)$$

Over the interval of $-\pi/2 < \omega_m t/2 < \pi/2$, $\theta(t) = \omega_m t/2$. While this definition is not valid outside the specified domain, we can derive an expression valid for all t by subtracting integral multiples of π such that $-\frac{\pi}{2} < \frac{\omega_m t}{2} - \kappa\pi < \frac{\pi}{2}$, where $\kappa \in \mathbb{Z}$. Using the floor operator $\lfloor . \rfloor$, κ can thus be expressed as:

$$\kappa = \left\lfloor \frac{\omega_m t}{2\pi} + \frac{1}{2} \right\rfloor \quad (9)$$

With the help of (9), we can express (8) for all t as:

$$\theta(t) = \frac{\omega_m t}{2} - \pi\left\lfloor \frac{\omega_m t}{2\pi} + \frac{1}{2} \right\rfloor \quad (10)$$

Now, realizing (7) is always nonnegative, we rewrite (5) as:

$$I_T(t) = \frac{I_{DC}}{2}\text{sgn}\left[\cos\left\{\left(\omega_H - \frac{\omega_m}{2}\right)t + \pi\left\lfloor \frac{\omega_m t}{2\pi} + \frac{1}{2} \right\rfloor\right\}\right] \quad (11)$$

Examining (11) in detail, we can expand the $\pi\lfloor . \rfloor$ term as:

$$\pi\left\lfloor \frac{\omega_m t}{2\pi} + \frac{1}{2} \right\rfloor = \begin{cases} 0 \text{ for } 0 \le t < \dfrac{\pi}{\omega_m} \\ x\pi \text{ for } \dfrac{(2x-1)\pi}{\omega_m} \le t < \dfrac{(2x+1)\pi}{\omega_m} \end{cases} \quad (12)$$

where $x \in \mathbb{Z}$.

Therefore, the $\pi\lfloor . \rfloor$ term adds a phase shift of π radians at $t = \pi/\omega_m$ seconds and an additional phase shift of π radians after every $2\pi/\omega_m$ seconds (at $t = 3\pi/\omega_m, 5\pi/\omega_m, \ldots$ seconds). Every time the phase shifts by π radians, it manifests as a sign change of $\frac{I_{DC}}{2}\text{sgn}\left[\cos\left\{\left(\omega_H - \frac{\omega_m}{2}\right)t\right\}\right]$. Thus, (11) can be equivalently represented in terms of the product of two signum functions:

$$I_T(t) = \frac{I_{DC}}{2} p_1(t) p_2(t) \quad (13)$$

where the functions $p_1(t)$ and $p_2(t)$ are defined as:

$$p_1(t) = \text{sgn}\left[\cos\left\{\left(\omega_H - \frac{\omega_m}{2}\right)t\right\}\right] \quad (14)$$

$$p_2(t) = \text{sgn}\left[\cos\left(\frac{\omega_m t}{2}\right)\right] \quad (15)$$

with $p_2(t)$ representing the effect of the $\pi\lfloor . \rfloor$ term in (11). Note that $p_1(t)$ and $p_2(t)$ are two square-waves alternating between ± 1 with constant (albeit different) frequencies, unlike $I_T(t)$ in (5). Therefore, it is possible to directly find the complex Fourier series of $p_1(t)$ and $p_2(t)$. Once we do that, it will allow us to compute the complex Fourier series of $I_T(t)$ with the simple application of the multiplication property of Fourier series [14].

IV. Fourier Series of Unbalanced Output Current

The complex Fourier series expansion of the square-waves $p_1(t)$ and $p_2(t)$ can be written as:

$$p_1(t) = \sum_{n=-\infty}^{\infty} C_n^{P1} e^{jn(\omega_H - \omega_m/2)t} \; ; \; p_2(t) = \sum_{n=-\infty}^{\infty} C_n^{P2} e^{jn(\omega_m/2)t} \quad (16)$$

$$C_n^{P1} = C_n^{P2} = \begin{cases} \dfrac{\sin(n\pi/2)}{n\pi/2} & for\ n \neq 0 \\ 0 & for\ n = 0 \end{cases} \quad (17)$$

To apply the multiplication property to $p_1(t)$ and $p_2(t)$, the fundamental frequencies of the two signals need be equal. Hence, we would like to express $p_1(t)$ and $p_2(t)$ in terms of the fundamental frequency of the sum of two sinusoids $f_c = \text{gcd}(f_L, f_H)$ [15], where gcd(.) is the greatest common divisor operator. To do so, we first define two frequency ratios in terms of the angular frequency ω_c as:

$$\alpha_H = \omega_H / \omega_c \; ; \; \alpha_L = \omega_L / \omega_c \quad (18)$$

where α_H and α_L are constant integers. This allows us to write:

$$p_1(t) = \sum_{k=-\infty}^{\infty} D_k^{P1} e^{jk(\omega_c/2)t} \; ; \; p_2(t) = \sum_{k=-\infty}^{\infty} D_k^{P2} e^{jk(\omega_c/2)t} \quad (19)$$

Recognizing that $\omega_c/2 = (\omega_H - \omega_m/2)(\alpha_H + \alpha_L)$, and also $\omega_c/2 = (\omega_m/2)(\alpha_H - \alpha_L)$, we define new complex Fourier coefficients D_k^{P1} and D_k^{P2} to make (19) equivalent to (16):

$$D_k^{P1} = \begin{cases} C_n^{P1} & for\ k = n(\alpha_H + \alpha_L) \\ 0 & otherwise \end{cases} \quad (20)$$

$$D_k^{P2} = \begin{cases} C_n^{P2} & for\ k = n(\alpha_H - \alpha_L) \\ 0 & otherwise \end{cases} \quad (21)$$

This is equivalent to zero-padding the complex Fourier series coefficients, inserting $(\alpha_H + \alpha_L)$ zeros between each sample in C_n^{P1} and $(\alpha_H - \alpha_L)$ zeros between each sample in C_n^{P2}.

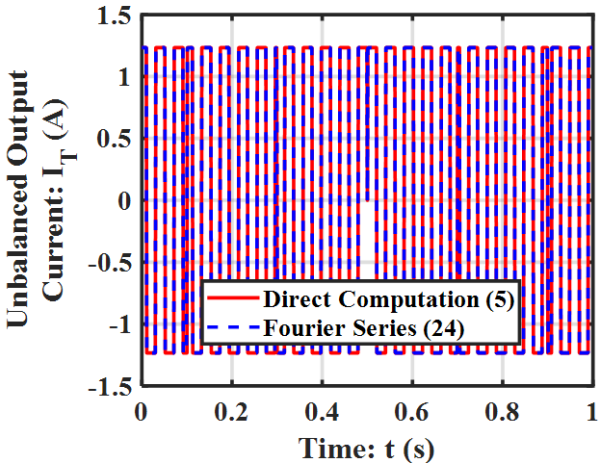

Fig. 2. Plot of unbalanced output current $I_T(t)$ for one time period $T_c = 1/f_c$ showing the equivalence of equations (5) and (24), assuming $I_{DC} \approx 2.5\ A$, $R_L = 100\ \Omega$, $f_H / f_L = 27/22.$. In (24), k is restricted from 1 to 10000.

Finally, the complex Fourier series coefficients of $I_T(t)$ can be calculated using convolution:

$$D_k^{IT} = D_k^{P1} * D_k^{P2} \quad (22)$$

$$I_T(t) = \frac{I_{DC}}{2} \sum_{k=-\infty}^{\infty} D_k^{IT} e^{jk(\omega_c/2)t} \quad (23)$$

Noting that $I_T(t)$ is even symmetric, D_k^{IT} is purely real. This implies $I_T(t)$ has the following trigonometric form:

$$I_T(t) = \frac{I_{DC}}{2} \sum_{k=1}^{\infty} 2D_k^{IT} \cos\left(\frac{k\omega_c t}{2}\right) \quad (24)$$

The validity of the derived Fourier series is confirmed by Fig. 2. Now we can use the complex Fourier series coefficients of $I_T(t)$ to derive expressions for the different current and voltages denoted in Fig. 1, which in turn, can be used to calculate DC power, RF output power, as well as efficiency.

V. Ideal Concurrent Class-D Voltages and Currents

Given that the load current $I_L(t)$ is the ideal brickwall filtered version of $I_T(t)$ at ω_L and ω_H, it can be expressed as:

$$I_L(t) = I_{DC} D_{kL} \cos(\omega_L t) + I_{DC} D_{kH} \cos(\omega_H t) \quad (25)$$

where $D_{kL} = D_{k=2\alpha_L}^{IT}$ and $D_{kH} = D_{k=2\alpha H}^{IT}$. Using Ohm's Law:

$$V_L(t) = R_L I_{DC} D_{kL} \cos(\omega_L t) + R_L I_{DC} D_{kH} \cos(\omega_H t) \quad (26)$$

$V_L(t)$ is then reflected across the transformer and is dropped across the transistors. Referring to the schematic shown in Fig. 1, the voltage drop across the transistor-side of the two transformers will be $V_{SN}(t) = V_{SP}(t) = V_L(t)/2$, where the factor 1/2 is due to the turns ratio of the transformers. The collector-emitter voltages can now be expressed as:

$$V_{CP}(t)=\begin{cases}0 & for\ V_{IP}(t)>0\\ -V_L(t) & for\ V_{IP}(t)<0\end{cases}\quad V_{CN}(t)=\begin{cases}V_L(t) & for\ V_{IP}(t)>0\\ 0 & for\ V_{IP}(t)<0\end{cases} \tag{27}$$

Notice that (27) represents two half-rectified versions of $V_L(t)$, with $V_{CP}(t)$ and $V_{CN}(t)$ coming from the negative and positive half-cycles respectively. We can express (27) more compactly using (14) and (15) as:

$$V_{CP}(t)=-V_L(t)\left[(1/2)-(1/2)\,p_1(t)\,p_2(t)\right] \tag{28}$$

$$V_{CN}(t)=V_L(t)\left[(1/2)+(1/2)\,p_1(t)\,p_2(t)\right] \tag{29}$$

Now using the equation for common-mode voltage from Fig. 1, $V_C(t)=V_{CN}(t)-V_{CP}(t)$, we can express $V_C(t)$ as:

$$V_C(t)=\frac{R_L I_{DC}}{2}\,p_1(t)\,p_2(t)[D_{kL}\cos(\omega_L t)+D_{kH}\cos(\omega_H t)] \tag{30}$$

As expected, $V_C(t)$ is the full-rectified version of $V_L(t)$, and its average value is V_{DC}. The complex Fourier series coefficients of the bracketed term in (30), using a common fundamental frequency of $\omega_c/2$ is:

$$D_k^{VL}=\begin{cases}D_{kL}/2 & for\ k=\pm 2\alpha_L\\ D_{kH}/2 & for\ k=\pm 2\alpha_H\\ 0 & otherwise\end{cases} \tag{31}$$

Using the results from (22) and (31), the multiplicative property can be applied to find the Fourier series coefficients of $V_C(t)$ as:

$$D_k^{VC}=D_k^{IT}*D_k^{VL} \tag{32}$$

Considering the even symmetry of $V_C(t)$, the Fourier series in trigonometric form is given as:

$$V_C(t)=R_L(I_{DC}/2)D_0^{VC}+R_L I_{DC}\sum_{k=1}^{\infty}D_k^{VC}\cos(k\omega_c t/2) \tag{33}$$

The DC voltage can be directly extracted from (33) as:

$$V_{DC}=(R_L/2)I_{DC}D_0^{VC} \tag{34}$$

VI. Ideal Concurrent Class-D Output Power and Drain Efficiency

The output RF power of the ideal concurrent dual-band push-pull class-D PA can be obtained directly using (25) as:

$$P_{RF}=I_{L,rms}{}^2R_L=(R_L/2)(I_{DC}D_{kL})^2+(R_L/2)(I_{DC}D_{kH})^2 \tag{35}$$

The total DC power consumed can be derived from (34) as:

$$P_{DC}=V_{DC}I_{DC}=(R_L/2)D_0^{VC}I_{DC}{}^2 \tag{36}$$

Finally, the drain efficiency can be calculated as:

$$\eta=P_{RF}/P_{DC}=(D_{kL}{}^2+D_{kH}{}^2)/D_0^{VC} \tag{37}$$

Looking back at (32) and using the commutative property of convolution, we can write:

TABLE I CALCULATION OF IDEAL CONCURRENT CLASS-D PA DC POWER, RF OUTPUT POWER AND DRAIN EFFICIENCY

f_H/f_L	I_{DC} (A)	R_L (Ω)	V_{DC} (V)	P_{DC} (W)	P_{RF} (W)	η
13/10	1.0000	6.0881	1.0000	1.0000	1.0000	**100%**
27/22	2.4674	100.00	40.529	100.00	100.00	**100%**
52/24	1.7447	2.0000	0.5732	1.0000	1.0000	**100%**

$$D_k^{VC}=D_k^{VL}*D_k^{IT}=\sum_{l=-\infty}^{+\infty}D_l^{VL}D_{k-l}^{IT} \tag{38}$$

Expanding the above summation for $k=0$, and realizing that since $I_T(t)$ is an even function, its Fourier series coefficients form an even sequence, we can further express:

$$\begin{aligned}D_0^{VC}=&D_{-2\alpha_L}^{VL}D_{2\alpha_L}^{IT}+D_{-2\alpha_H}^{VL}D_{2\alpha_H}^{IT}\\ &+D_{2\alpha_L}^{VL}D_{2\alpha_L}^{IT}+D_{2\alpha_H}^{VL}D_{2\alpha_H}^{IT}\end{aligned} \tag{39}$$

Finally, using (25) and (31), we can write $D_0^{VC}=D_{kL}{}^2+D_{kH}{}^2$, and thus, from (37), $\eta=1\equiv 100\%$. Alternatively, MATLAB simulation results for different ratios of f_H/f_L are demonstrated in Table 1 to show 100% theoretical efficiency.

VII. Validation of Theory

To further establish the usefulness of the above analysis, we validate it against results obtained from [8]. The authors of [8], using largely numerical and empirical methods, claimed that the common mode voltage (V_C in the current paper) of a concurrent dual-band class-D PA has large second order intermodulation (IM2) components and showed that terminating these components with high impedances (which implicitly holds true for an ideal transformer balun but not necessarily for even an ideal distributed balun) is mandatory for achieving high efficiency. Here, we use (33) to analytically

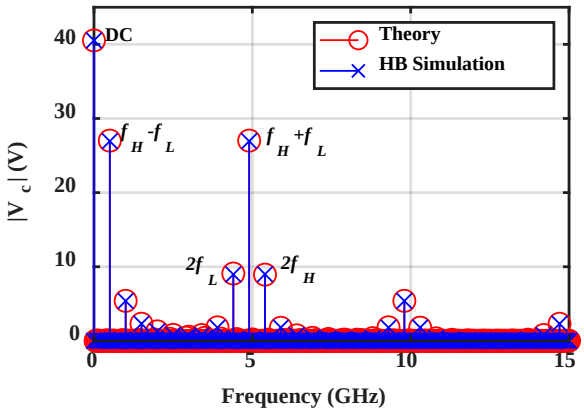

Fig. 3. Magnitude of complex Fourier series coefficients of the balun common-mode voltage, showing large IM2 components, derived analytically (red), and using Harmonic Balance simulation (blue), for $I_{DC}\approx 2.5\ A$, $R_L=100\ \Omega$, $f_L=2.2$ GHz, $f_H=2.7\ GHz$. The overlap between the two plots demonstrates the agreement between theory and simulation.

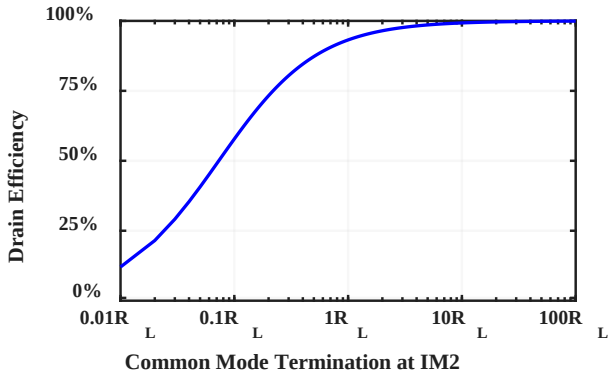

Fig. 4. Plot showing the deterioration of drain efficiency of an ideal concurrent dual-band class-D PA, derived analytically, as the common mode termination impedance at the two IM2 frequencies is decreased, assuming $I_{DC} \approx 2.5\ A$, $R_L = 100\ \Omega$, $f_H / f_L = 27/22$.

compute the complex Fourier series coefficients of $V_C(t)$. In Fig. 3, the magnitude of these coefficients, obtained analytically, is plotted using red lines, illustrating large IM2 components, as envisaged in [8]. Furthermore, Fig. 4 shows the degradation of drain efficiency as the termination impedance of $V_C(t)$ is lowered, which aligns with the empirical observation of [8].

We also verify the theoretically derived magnitude of the complex Fourier series coefficients of $V_C(t)$ against Harmonic Balance simulation results from Keysight Advanced Design System (ADS). An ideal concurrent dual-band Class D PA is designed to operate at $f_L = 2.2$ GHz and $f_H = 2.7$ GHz, with I_{DC} approximately 2.5 A and $R_L = 100\ \Omega$. The number of harmonics for both tones as well as the maximum number of mixing order are set to 50 and the resulting magnitude spectrum of $V_C(t)$ is plotted using blue lines in Fig. 3. It can be observed that the theoretical and simulation results overlap, further supporting the analysis presented in this paper.

VIII. Conclusion

This paper developed a new technique to theoretically compute the complex Fourier series of signals in a concurrent dual-band system. With the use of the analysis it has derived the ideal drain efficiency of a concurrent dual-band class-D PA is 100%. The calculated Fourier coefficients are also used to develop insights about common-mode termination requirements of the PA, which are seen to be in line with empirical observations from literature. In future, the analysis can be advanced to include other nonidealities so that more insights can be generated about concurrent dual-band class-D operation. Also, the analysis in this paper can be adapted to provide insights into the operation of other concurrent dual-band systems, in particular, those involving nonlinear distortion of a sum of sinusoids.

References

[1] "Carrier Aggregation explained." [Online]. Available: https://www.3gpp.org/technologies/keywords-acronyms/101-carrier-aggregation-explained. [Accessed: 29-Jan-2020].

[2] "Specification # 38.716-01-01." [Online]. Available: https://portal.3gpp.org/desktopmodules/Specifications/SpecificationDetails.aspx?specificationId=3516. [Accessed: 29-Jan-2020].

[3] X. Chen, W. Chen, F. M. Ghannouchi, Z. Feng, and Y. Liu, "Enhanced Analysis and Design Method of Concurrent Dual-Band Power Amplifiers With Intermodulation Impedance Tuning," IEEE Trans. Microw. Theory Tech., vol. 61, no. 12, pp. 4544–4558, Dec. 2013.

[4] Y. Li, B. J. Montgomery, and N. M. Neihart, "Development of a concurrent dual-band switch-mode power amplifier based on current-switching class-D configuration," in 2016 IEEE 17th Annual Wireless and Microwave Technology Conference (WAMICON), 2016, pp. 1–4.

[5] J. Pang, S. He, C. Huang, Z. Dai, C. Li, and J. Peng, "A Novel Design of Concurrent Dual-Band High Efficiency Power Amplifiers With Harmonic Control Circuits," IEEE Microw. Wirel. Compon. Lett., vol. 26, no. 2, pp. 137–139, Feb. 2016

[6] R. Kalyan, K. Rawat, and S. K. Koul, "Design strategy of concurrent multi-band Doherty power amplifier," IET Microw. Antennas Amp Propag., vol. 9, no. 12, pp. 1313–1322, Jul. 2015.

[7] Z. Zhang, Y. Li, and N. M. Neihart, "Architecture comparison for concurrent multi-band linear power amplifiers," in 2015 IEEE 58th International Midwest Symposium on Circuits and Systems (MWSCAS), 2015, pp. 1–4.

[8] B. Montgomery, Y. Li, and N. M. Neihart, "Common-mode termination requirements in concurrent dual-band push-pull power amplifiers," in 2017 IEEE International Symposium on Circuits and Systems (ISCAS), 2017, pp. 1–4.

[9] S. C. Cripps, RF Power Amplifiers for Wireless Communications, 2nd ed., vol. 2. Artech House Microwave Library, 2006.

[10] A. Grebennikov, N. O. Sokal, M. J. Franco, Switchmode RF and Microwave Power Amplifiers. Academic Press, 2012.

[11] J. W. Strutt, 3rd Baron Rayleigh, The theory of sound, vol. 1. Macmillan and Co., 1877.

[12] M. Albulet, RF Power Amplifiers, vol 2. SciTech Publishing, 2001.

[13] L. M. A. Aguilar, C. Robledo-Śanchez, M. L. A. Carrasco, and M. M. Méndez Otero, "The principle of superposition for waves: The amplitude and phase modulation phenomena," 2012.

[14] S. Haykin, B. Van Veen, Signals and Systems. John Wiley & Sons, 2007.

[15] D. Sundararajan, Fourier Analysis—A Signal Processing Approach. Springer, 2018, pp. 179–216.